541. Smart optical rotation speed transducer

P. Kuzas[1], V. Augutis[2]
[1,2] Kaunas University of Technology,
Studentu 50-445, LT-51368, Kaunas, Lithuania
E-mail: [1] *Pranas.Kuzas@stud.ktu.lt*, [2] *Vygantas.Augutis@ktu.lt*

(Received 11 December 2009; accepted 07 June 2010)

Abstract. This paper presents a transducer that was designed for rotation speed measurement of water meter impeller during verification procedure of counting mechanisms. In many cases, particularly when wet type water meters are verified, the impeller is obstructed by dregs, rust, etc. and therefore is hardly visible. When using filtration both in spatial and frequency domains, steady and reliable measurements are obtained. Both theoretical and experimental results are presented in this paper. In this research work transfer function of smart rotational speed measurement transducer is shown and various modes of input parameters are modeled. The reliability of the transducer output signal and its response to optical disturbances are modeled and real signals from transducer prototype are given.

Keywords: rotation speed, measurement, smart transducers, spatial filters.

Introduction

In engineering practice the rotation speed and its instability measurements must be conducted often. The rotating objects may be star-shaped patterns, propellers, water meter counting mechanisms. Also rotating objects with irregular shapes can occur. The rotating object can be obstructed due to various reasons. In some cases the only way to determine the rotation speed of the object is to implement optical transducers. This is very important in automatic evaluation procedure of counting mechanisms of wet type water meters. The rotating impeller of this type of counters is obstructed by rust, dregs, bubbles, which accumulate on the glass of the counting mechanism.

In fig. 1 the wet type water meter impeller is presented. In installation conditions (fig. 1a) the clear visibility of impeller is disturbed by:

1. Impeller‘s optical surface quality
2. Impeller‘s geometry
3. Impeller‘s eccentricity
4. Side effects of insufficient filtering of water (bubbles, rust, dregs, etc.)

Measurement object

All the problems mentioned above cause reflective transducers with single sensing element to fail. The purpose of the proposed transducer is measuring the rotation speed. The transfer function:

$$F = \phi(\Omega), \qquad (1)$$

where F – the frequency of the signal measured in the output stage of the transducer (Hz), Ω - impeller’s rotation speed (rps).

When the impeller’s blades are situated periodically, following the circle line, the function is:

$$F = N\Omega\,. \qquad (2)$$

“Smart” transducer must ensure the stability of the transfer function. The correlation function for that requirement was chosen [2,3]. The software implementation of correlation procedure is time and computing resources consuming [6] and requires the speed of image capturing and processing hardware. These restrictions were taken into account and hardware implementation of correlation function was chosen. The model of the hardware implementation is given below.

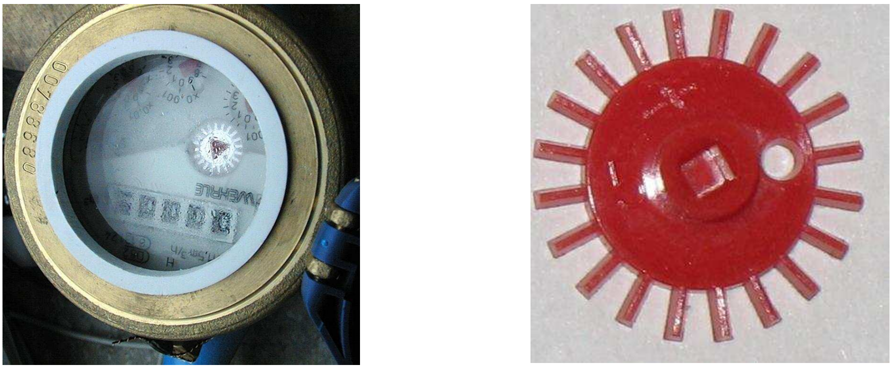

a) b)

Fig. 1. Wet type water meter counting mechanism and the rotating impeller

Model of the transducer

The image of impeller is projected on the receiver plane, using optic lens. This image (Fig.2) can be de-scribed as:

$$\phi = \sum_{k=1}^{N} \phi_k(\rho,\varphi), \qquad \begin{matrix} R1 < \rho < R2; \\ 2(N-1)\dfrac{\pi}{N} < \varphi < (2N-1)\dfrac{\pi}{N}; \end{matrix} \qquad (3)$$

where k – number of the blade, N – amount of the blades, Ω – angular speed of rotation, $R1$, $R2$ – radiuses, ρ,φ – polar coordinates.

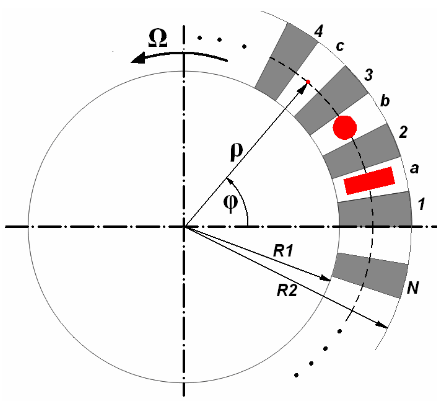

Fig. 2. Image projection

Type and shape of the surface of the sensitive element can be different (photo transistor, photodiode, photo resistor). Let's analyze these cases as it is shown in fig. 2. In case "a" the shape of the sensitive element coincides with the shape of the blade. In case "b" the sensor area is circular. This sensitive area touches edges of the blade projection. In case "c" the sensitive element is much smaller than blade width. The area occupied by sensitive element is relatively small and can be treated as point. When blades pass these elements, the signals $u(\alpha)$ are obtained. Possible forms of these signals are shown in fig. 3. Here α – normalized angle.

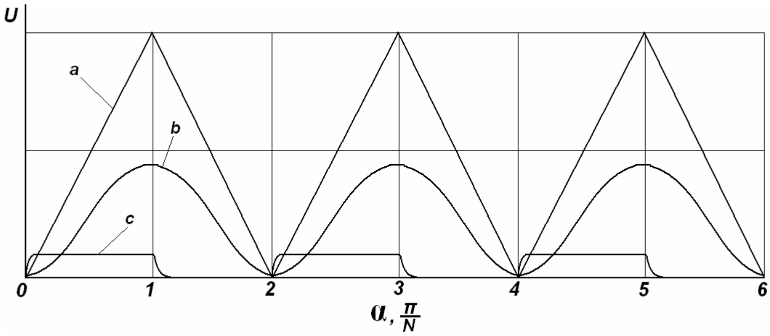

Fig. 3. Shape of signals obtained from sensitive element shapes a, b and c

In case "a" the output signal shape is triangular, in case "c" the shape is close to rectangular. In case "b" signal shape is close to:

$$u(\alpha) = \left(1 - \alpha^2\right)^{\frac{1}{2}} + \arcsin(\alpha). \qquad (4)$$

In all cases phase modulation will be present due to impeller eccentricity. The frequency of modulation is equal to angular speed of rotation Ω. Furthermore, in cases "a" and "b", the amplitude modulation exists.

With purpose to diminish impact of eccentricity, as well as impact of brightness of blades and inequality of sensitivity of sensitive elements, a set of *N* elements is used. Sensitive elements are situated at equal distances, following the circle, which radius falls between *R1* and *R2*. Output signal from sensitive elements is:

$$u(\alpha) = K \sum_{k=1}^{N} \int_{R1}^{R2} \int_{0}^{\alpha} S(\rho, \varphi) \Phi_k(\rho, \varphi) d\rho d\varphi., \qquad (5)$$

In this formula, the assumption is made that sensitivity and area of each element are equal. This condition can be fulfilled by choosing sensitive elements with equal characteristics. In order to evaluate the influence of eccentricity on impeller rotation speed measurement, the digital modeling was performed. For modeling purposes the model was developed which is based on expression (5).

Modeling results

Using model based on (5), the transducer response to the optical surface of the impeller was simulated. Single element response was modeled and compared to 20 elements summed response. The shapes of sensitive optical element were used as mentioned above:

1. Point – shaped
2. Circular
3. Rectangular

Also the eccentricity of 1 mm., which is more than maximum eccentricity in water counter mechanism impeller, was simulated. The output signal and it‘s spectrum were calculated for „ideal“ image (fig. 4a) and for image with various types of optical noise (fig. 4b).

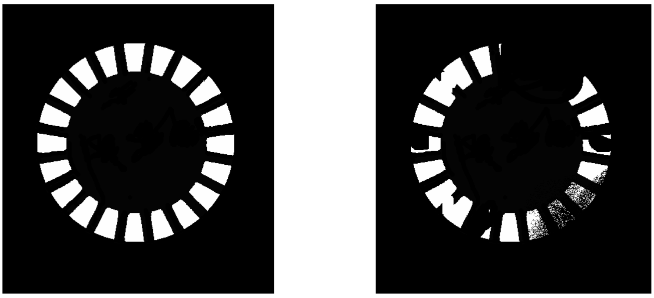

a) b)

Fig. 4. Optical surface images for digital model

The comparison was performed both in time and in frequency domain. The ideal and noisy images were put under equal simulating conditions and simulation was carried out as follows:

1. No eccentricity, point – shaped sensitive element
2. Eccentricity of 1 mm., point – shaped element
3. No eccentricity, circular sensitive element
4. Eccentricity of 1 mm., circular element
5. No eccentricity, rectangular sensitive element
6. Eccentricity of 1 mm., rectangular element

Typical time and frequency domain signals obtained from simulations are demonstrated in Fig. 5-12. Single element response and combination of 20 sensitive elements response to test images are shown. Model was programmed using Delphi as programming environment.

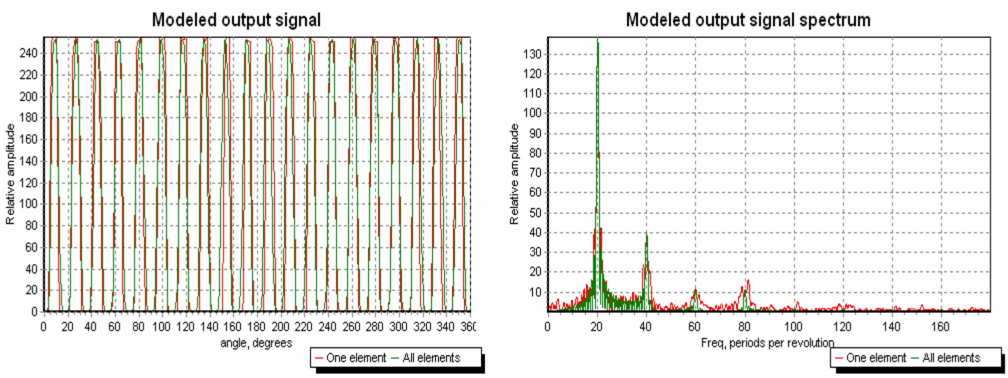

Fig. 5. Modeled output signal from point-shaped elements over “ideal” image

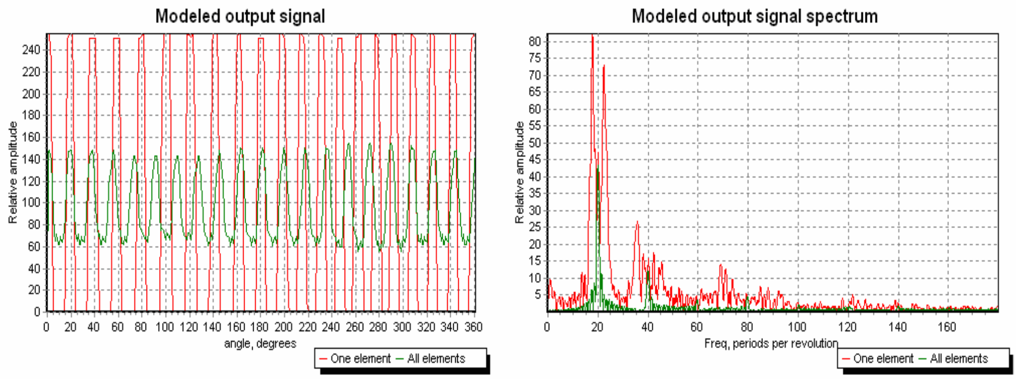

Fig. 6. Modeled output signal from point-shaped elements over “ideal” image, eccentricity 1 mm.

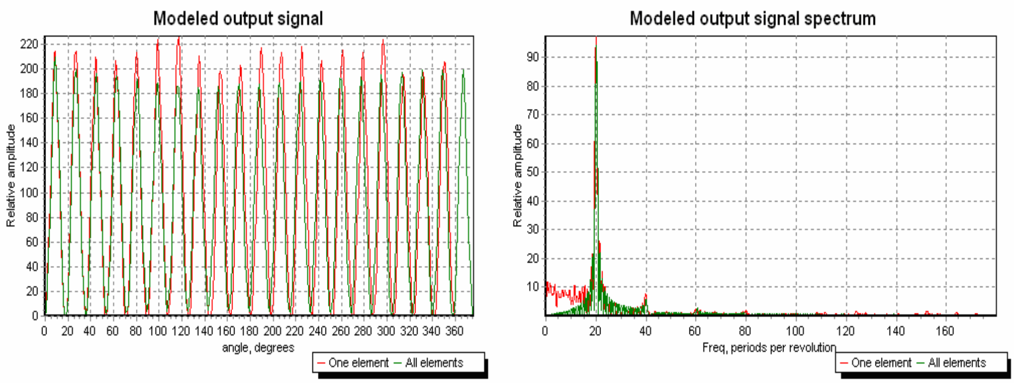

Fig. 7. Modeled output signal from circular elements over “ideal” image

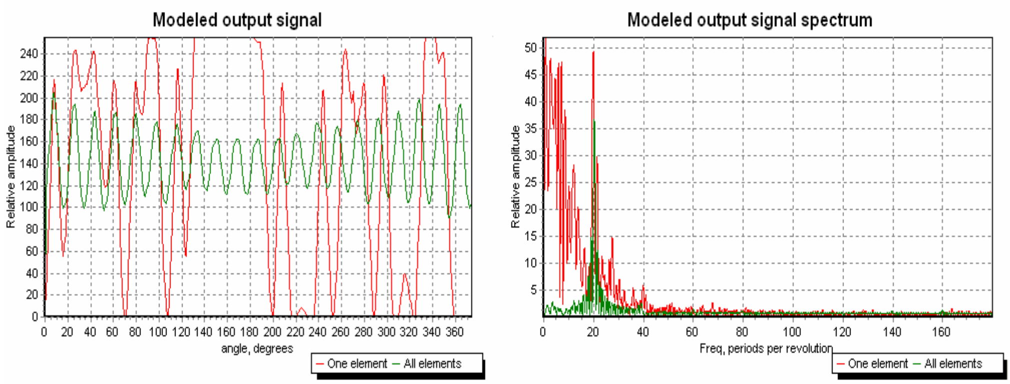

Fig. 8. Modeled output signal from circular elements over “noisy” image

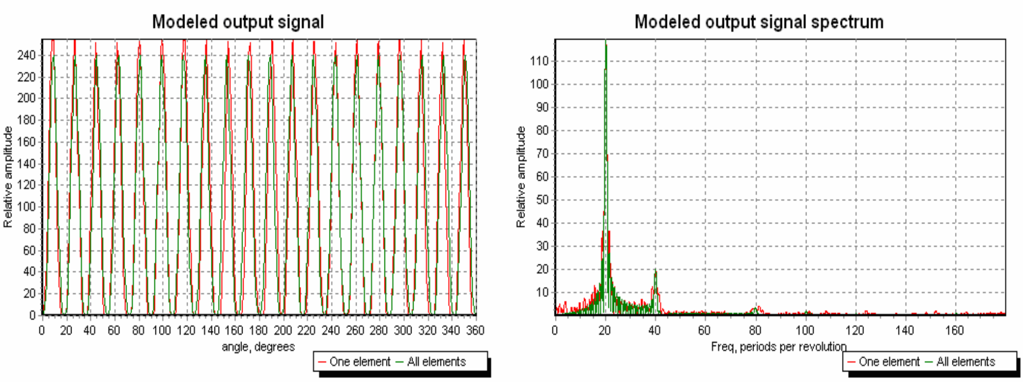

Fig. 9. Modeled output signal from rectangular elements over “ideal” image

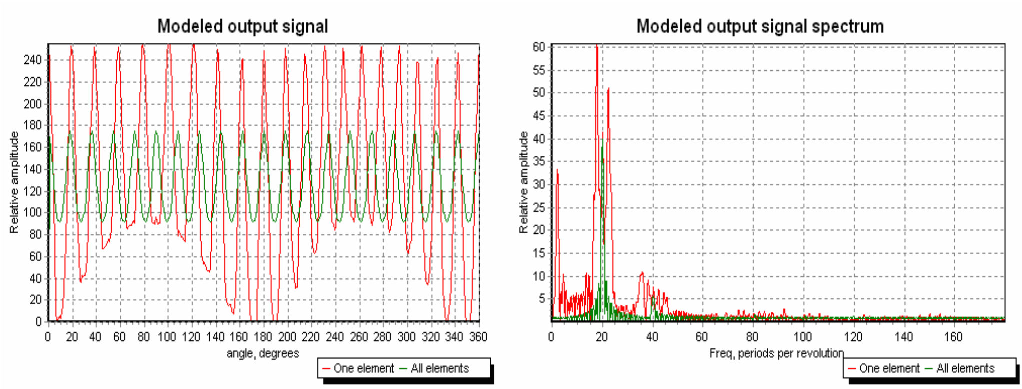

Fig. 10. Modeled output signal from rectangular elements over “ideal” image, eccentricity 1 mm**.**

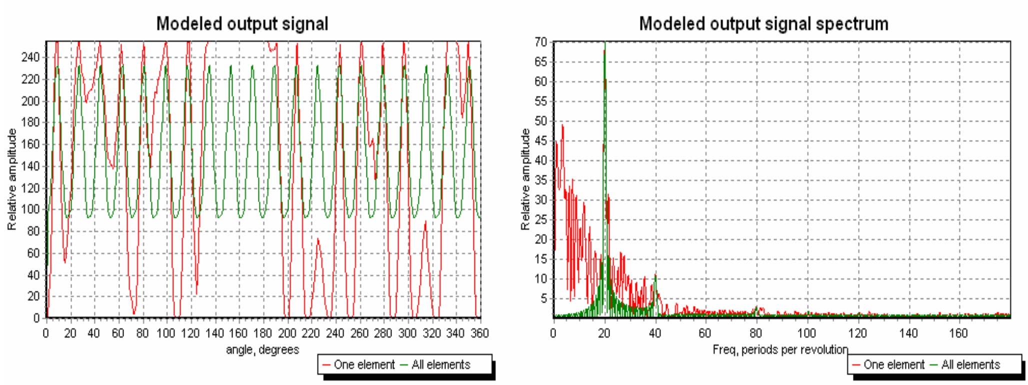

Fig. 11. Modeled output signal from rectangular elements in noisy image

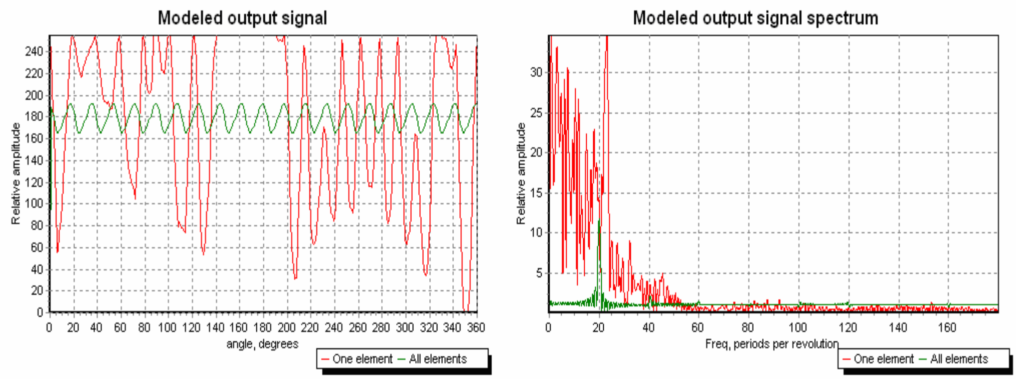

Fig. 12. Modeled output signal from rectangular elements in noisy image, eccentricity 1 mm.

Modeling conclusions:

From modeling results the following considerations can be formulated:

1. As it was expected, using N receivers instead of one, enables elimination of influence of eccentricity of the impeller. This is obvious from spectrum of the signals. Furthermore, as it is visible in figures 8, 10, 11 and 12 the influence of disturbances is significantly reduced.
2. According to measurement problem, which is solved using smart optical transducer, the output signal can be processed using one of the following algorithms:
    a. If rotating speed of the impeller upper and lower limits are known, and these limits are up to 10 %, the pass band filter with narrow band can be used to select the informative part of the signal. The measuring time is several periods of transducer output signal. The maximum speed of measurement can be achieved in this way. The eccentricity elimination is minimal when *N* periods of output signal are measured.
    b. When rotating speed of the impeller changes in wide range, also when disturbances in optical part are large, the FFT analysis of the output signal must be conducted. The impeller rotating speed is then calculated as position of peak of the FFT function.

Experiment

After optimization, and design considerations [1], the real transducer was constructed and signals were visualized under various conditions. Signals from optical transducer and their spectrums are shown in fig. 12-14. Tektronix TDS 2014 digital storage oscilloscope and software written under Matlab were used for signal acquisition. The transducer construction is shown in fig. 13.

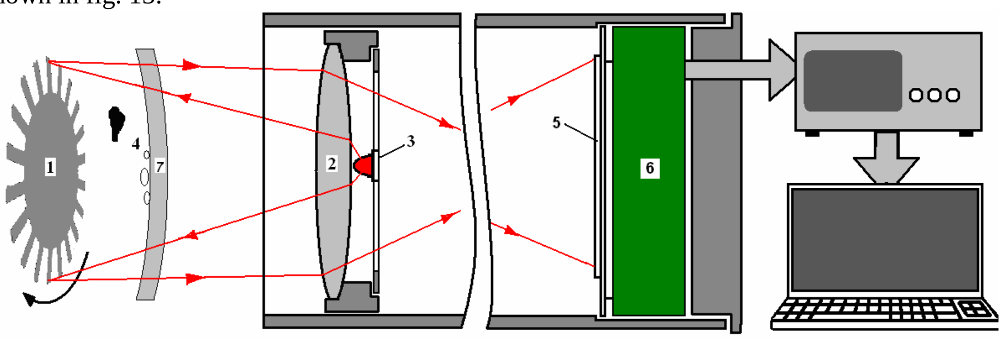

Fig. 13. The construction of the smart rotational speed transducer and test circuit

Optical surface is projected to spatial filter 5 through water counter front glass 7 and optical transducer lens 2. The visibility of the impeller is obstructed by dregs, rust and bubbles (4). The filtered signal is captured by signal acquisition board 6. Subsequently, the signal is fed into oscilloscope, which is linked to the computer with signal processing software. The normalized power spectrum is given in figures 14 – 16 in comparison with time domain signal. K=1 means the whole spectrum energy under ideal visibility.

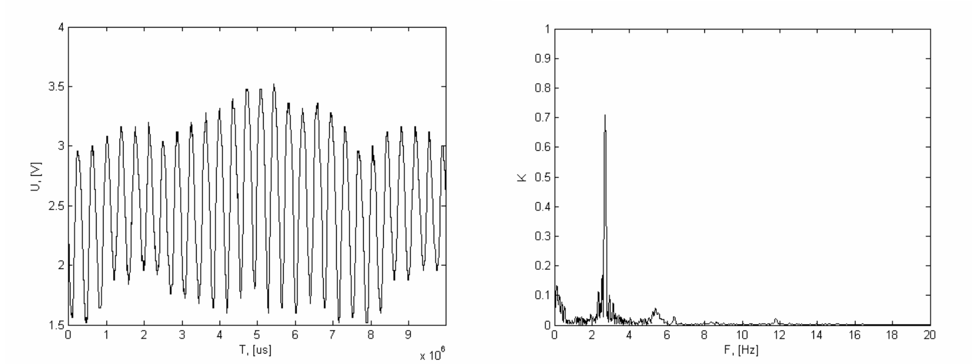

Fig. 14. Output signal from smart transducer and it's spectrum. Full visibility of the impeller, frequency from blades is 2,6 Hz

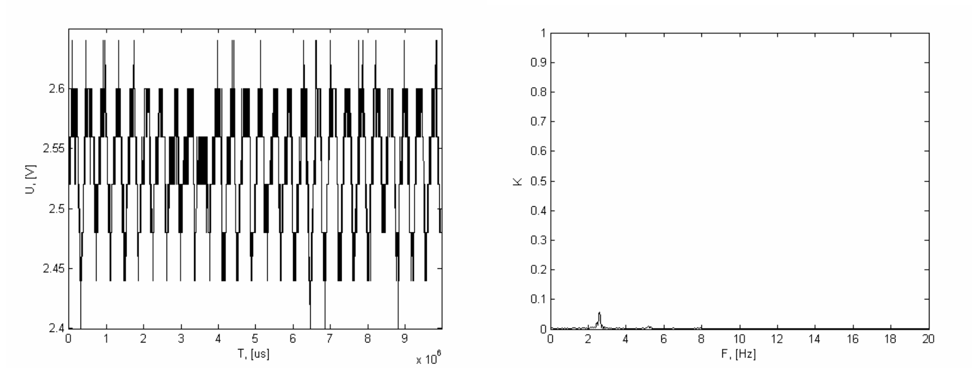

Fig. 15. Output signal from smart transducer. Visibility of blades < 5 %, frequency from blades is 2,6 Hz

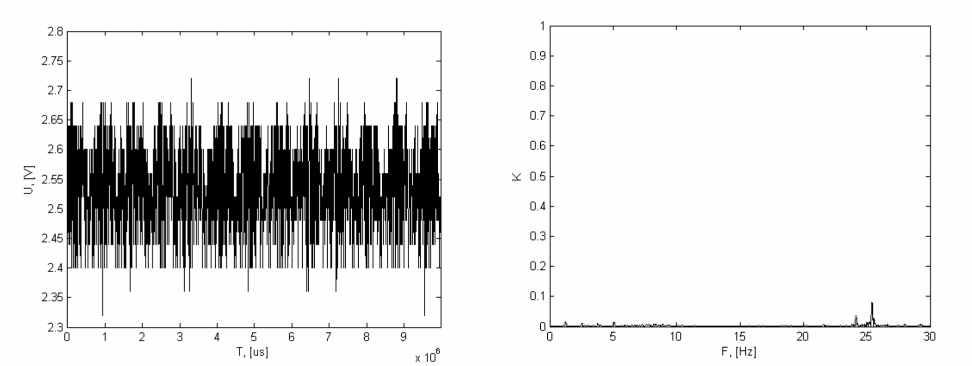

Fig. 16. Output signal from smart transducer. Visibility ~25 %, frequency from blades is 25 Hz

Conclusions:

Smart rotation speed transducer, based on spatial filter was developed. Simulated and actual signals indicate that spatial filter significantly increases the signal to noise ratio when working in noisy conditions. The solution based on discrete elements allows capturing signals from impellers up to 250 Hz. Discrete elements can be formed virtually using captured images from the digital camera, so the rotational speed can be calculated for irregular shapes.

References

1. **Латыев С. М.,** Конструирование точных оптических приборов, «Политехника», Санкт - Петербург, 2007, с. 581.
2. **Старк Г.,** Применение методов Фурье-оптики, «Радио и связь», Москва, 1988, с. 536.
3. **Vijaya Kumar B. V. K., Mahanalobis A., Juday R.,** Correlation Pattern Recognition, Cambridge, p. 404. Online: http://www.cambridge.org/catalogue/catalogue.asp?isbn=9780521571036
4. **Giniotis V.** Position and Displacement Measurement. Vilnius: Technika, 2005, p. 215 (Padėties ir poslinkių matavimas) (in Lithuanian).
5. **Giniotis V., Grattan K. T. V.,** Optical Method for the Calibration of Raster Scales, Measurement, 32/1, 2002, pp. 23-29.
6. **Augutis V., Gailius D., Kuzas P.** Low Cost Microscope Add-On System for Subpixel Resolution Displacement Measurement 2007 IEEE Instrumentation and Measurement Technology Conference Proceedings ISSN: 1091-52.